

RESEARCH ARTICLE | JANUARY 23 2023

Purcell enhanced single-photon emission from a quantum dot coupled to a truncated Gaussian microcavity

Lena Engel ; Sascha Kolatschek ; Thomas Herzog ; Sergej Vollmer; Michael Jetter ; Simone L. Portalupi ; Peter Michler 

 Check for updates

Appl. Phys. Lett. 122, 043503 (2023)

<https://doi.org/10.1063/5.0128631>



View
Online



Export
Citation

CrossMark



 CryoComplete

A total solution for low-temperature characterization

[Learn more >](#)



Purcell enhanced single-photon emission from a quantum dot coupled to a truncated Gaussian microcavity

Cite as: Appl. Phys. Lett. **122**, 043503 (2023); doi: [10.1063/5.0128631](https://doi.org/10.1063/5.0128631)

Submitted: 29 September 2022 · Accepted: 13 December 2022 ·

Published Online: 23 January 2023



View Online



Export Citation



CrossMark

Lena Engel,^{a)}  Sascha Kolatschek,  Thomas Herzog,  Sergej Vollmer, Michael Jetter,  Simone L. Portalupi,  and Peter Michler 

AFFILIATIONS

Institut für Halbleiteroptik und Funktionelle Grenzflächen, Center for Integrated Quantum Science and Technology (IQST) and SCOPE, University of Stuttgart, Allmandring 3, 70569 Stuttgart, Germany

^{a)} Author to whom correspondence should be addressed: l.engel@ihfg.uni-stuttgart.de

ABSTRACT

Purcell enhancement of quantum dot (QD) single-photon emission and increased device brightness have been demonstrated with various types of microcavities. Here, we present the first realization of a truncated Gaussian-shaped microcavity coupled to a QD. The implementation is based on wet-chemical etching and epitaxial semiconductor overgrowth. The cavity modes and their spatial profiles are experimentally studied and agree well with simulations. The fundamental mode wavelength with Q-factors around 6000 and a small polarization splitting of 29 μeV can be reproducibly controlled via fabrication design, enabling the adaption of the cavity to a specific QD. Finally, transitions of a QD inside a cavity are tuned on and off resonance via temperature tuning. A reduced decay time by a factor above 3 on resonance clearly indicates Purcell enhancement while second-order correlation measurements of $g^{(2)}(0) = 0.057$ prove that the QDs single-photon characteristic is preserved.

Published under an exclusive license by AIP Publishing. <https://doi.org/10.1063/5.0128631>

Semiconductor quantum dots (QDs) have proven to be promising candidates for the realization of bright on-demand single-photon sources with a high degree of indistinguishability.^{1,2} To be suited for practical applications,^{3–5} ideally every photon emitted by a QD should be extracted and collected. However, the extraction efficiency of semiconductor QDs is limited due to the high refractive index contrast at the semiconductor to air interface.⁶ To overcome this limitation, several geometric designs, including printed or etched microlenses,^{7,8} solid immersion lenses,⁹ nanowires,¹⁰ and photonic trumpets,¹¹ are under investigation. Other approaches are quantum cavity electrodynamic (QCED) based systems like micropillars,^{12,13} microdisks,¹⁴ fiber-coupled Fabry-Pérot cavities,¹⁵ circular Bragg gratings,^{16,17} and photonic crystal cavities,^{18,19} which utilize the Purcell effect to increase the brightness of semiconductor QDs and shorten the lifetime, thus enabling higher repetition rates.²⁰

An intensively studied and very intuitive way of realizing a planar Fabry-Pérot cavity in semiconductor materials is planar Bragg cavities,²¹ which consist of two distributed Bragg reflectors (DBRs). To achieve in-plane confinement, a mesa-like structure can be implemented into the top DBR. This has been theoretically and experimentally shown with etched mesa-structures for polaritons.^{22,23} For

smoother in-plane confinement and, thus, improved quality factor of the cavity, Ding and coworkers proposed the substitution of the mesa inside the cavity with a Gaussian-shaped structure.²⁴ So far, cavities containing a nano-scale Gaussian-shaped defect have been fabricated in the $\text{Ta}_2\text{O}_5/\text{SiO}_2$ material system.²⁵ However, the realization in the GaAs material system and, thus, the possibility to embed QDs is still outstanding.

In this work, we present the realization of truncated Gaussian-shaped microcavities coupled to single QDs for enhanced single-photon emission in a semiconductor system. The robust design, in principle, allows for fabrication of microcavity membrane structures that promise the possibility of employing strain tuning²⁶ as well as the implementation of additional optics directly on the sample surface. The monolithic implementation of this structure is enabled by epitaxial overgrowth of a wet-chemically etched truncated Gaussian-shaped microlens with a top DBR. We describe the fabrication process, regarding etching and chemical and thermal oxide removal as well as the asymmetric DBR growth. The optical and spatial properties of the fundamental as well as higher order cavity modes are precisely measured by performing in-plane micro-photoluminescence ($\mu\text{-PL}$) scans over one cavity showing excellent agreement with simulations.

We show that varying the aspect ratio of the Gaussian structure by changing the etching mask diameter shifts the resonance wavelength of the cavity. In future, this will allow for adaption to preselected QDs in a deterministic fabrication process. Finally, Purcell enhancement is shown by tuning QD emission lines on resonance with the cavity via temperature variation.

The sample design can be seen in Fig. 1. 30 pairs of alternating aluminum arsenide (AlAs) and gallium arsenide (GaAs) layers are grown via metal-organic vapor-phase epitaxy (MOVPE) forming the bottom DBR. The self-organized indium arsenide (InAs) QDs are embedded in a λ -thick GaAs layer.

In the first step of processing, the position and diameter of the microlenses are determined via photolithography, which is used to expose disk-shaped structures in the resist. For this purpose, two different methods are used in this work. The first is hard mask lithography. This technique allows for the fast realization of multiple arrays of structures, where the disk diameter is constant, while the following processing parameters can be studied and varied. This allows for gaining statistics on the cavity geometry and optimization of the subsequent processing steps. The second approach is based on laser lithography with which structures with variable diameter can be easily exposed to optimize the geometry with regard to finite-difference time-domain (FDTD) simulations. Second, silicon dioxide (SiO_2) is deposited using electron-beam physical vapor deposition, so that after the following lift-off process, circular disks remain on the sample surface. The hereby defined SiO_2 disks serve as etching masks during the following wet-chemical etching process in an aqueous solution of sulfuric acid (H_2SO_4) and hydrogen peroxide (H_2O_2).²⁷ Figure 1(a) shows a schematic of the circularly shaped hard mask during wet-

chemical etching. Due to the isotropy of the etching process in combination with capillary effects at the edges of the masks, Gaussian-shaped microlenses are formed. As described in Ref. 28, the aspect ratio of the microlenses can be designed deterministically by assigning the etching time and disk diameter. QDs outside of the lens become optically inactive due to their proximity to the etched surface [as schematized in Fig. 1(a)]. At the end of the etching process, the disks are removed mechanically by carefully wiping them off so that the cavity thickness of 1λ is preserved in the center region as it is shown in Fig. 1(b). Atomic force microscopy (AFM) measurements confirm the Gaussian shape of the microlenses sidewalls as well as a surface roughness of 0.3 ± 0.2 nm on top of and 0.4 ± 0.2 nm between the lenses. These values are comparable to epi-ready wafers; thus, overgrowth on this structured surface is possible. To ensure homogeneous overgrowth, free of defects, the sample is treated with pure sulfuric acid to remove oxides from the surface before inserting it into the growth reactor where an extended pre-heating step is performed to remove residual oxides directly before growth. The microlenses are thereafter overgrown with a GaAs spacer layer with appropriate thickness. The cavity is completed by 20 pairs of top DBR favoring emission to the upper direction as it is sketched in Fig. 1(c). A scanning electron microscopy (SEM) cross section of a realized structure is depicted in Fig. 1(d). The Gaussian-shape of the sidewalls that allows for smooth in-plane confinement can be seen. The center part of the cavity shows a plateau that does not influence the general cavity characteristics and performance significantly. Therefore, the final shape is the one of a truncated Gaussian. Due to the different growth rates of the top DBR materials along the distinct crystal axis,²⁹ the final cavities become slightly elliptical with increasing height [the inset of Fig. 1(d)].

For the optical measurements, a confocal μ -PL setup is used with the sample mounted inside a liquid helium bath cryostat and cooled down to 4 K. To characterize the cavity modes, an above-band continuous wave (cw) excitation at ~ 650 nm is used. For a detailed analysis of the mode structure, one cavity is selected. By performing a two-dimensional in-plane scan over the cavity, spectra can be obtained at different positions of the cavity.³⁰

In Fig. 2(a), all measured spectra are plotted in a single graph. A polarization series of the fundamental cavity mode shows a small splitting of the polarization eigenmodes of $29 \mu\text{eV}$, a clear sign for a slight ellipticity of the structure that can also be seen by viewing the top part of the cavity [see the inset in Fig. 1(d)]. To obtain the spatial profile of the mode intensity, the corresponding spectral peak is filtered through a monochromator, and the signal is sent to an avalanche photodiode (APD) while performing the same two-dimensional scan mentioned above. At 893.05 nm, the fundamental mode of the cavity can be seen with a Gaussian-shaped mode profile [see the image labeled 1 in Fig. 2(b)]. For shorter wavelengths, the visible higher order transverse modes exhibit a clear signature of Hermite–Gaussian modes. To validate that these measurements of the propagating field indeed represent the distribution of the near-field, FDTD simulations are performed. For the simulations, an ideal Gaussian form with an ellipticity of around 10% is chosen to get a clear separation of the modes. As seen in Figs. 2(b) and 2(c), a close resemblance between the simulated near-field and the measured propagating field can be observed. For the third order modes (3.1 and 3.3), the Hermite–Gaussian modes are, in principle, identical except for a 90° rotation. The small deviation of the measurements as well as the simulations from this ideal form stem

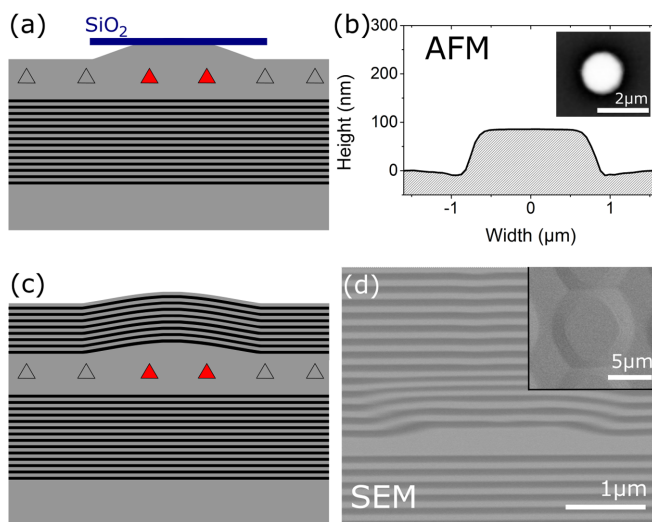


FIG. 1. (a) Schematic cross section of the microlens during the wet-chemical etching process with the SiO_2 etching mask on top. The positions of the QDs are depicted as triangles. Non-colored QDs have become inactive during processing due to their proximity to the etched surface. (b) AFM profile of a Gaussian-like shaped lens after the etching process before overgrowth (without SiO_2 disks). The cavity thickness of 1λ is preserved in the flat center region. The inset shows the 2D data indicating rotation symmetry. (c) Schematic cross section of the final microcavity. (d) SEM cross section and top view (inset) of the cavity.

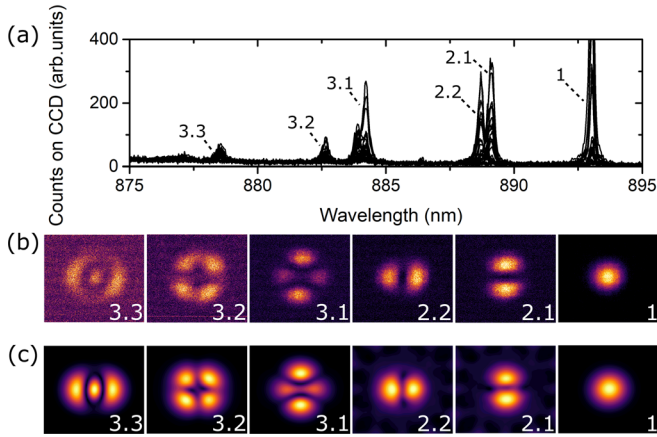


FIG. 2. (a) μ -PL spectra obtained at different positions of one cavity by performing a two-dimensional in-plane scan. The measured (b) and simulated (c) mode profiles are displayed below. The inset numbers correspond to those of the resonance peaks depicted in (a).

from a non-perfect spectral selection of the cavity mode while performing the two-dimensional scan.

In a next step, a closer investigation of the fundamental cavity mode is performed. For this purpose, cavities on the basis of varying SiO₂ disk diameters are fabricated. Once overgrown, the resulting dependence of the fundamental mode spectral position from the disk diameter as seen in Fig. 3 shows a similar behavior to micropillar cavities.³¹ The realized cavities exhibit Q-factors between 5000 and 7000 proving the effectiveness and reproducibility of the fabrication process. In deterministic fabrication, the control of the cavity mode wavelength during fabrication is fundamental for successful spectral matching between the preselected emitter and realized cavity. Hence, the SiO₂ disk diameters can serve as a tuning knob to achieve the required spectral control.

An important figure of merit of a cavity is the Purcell enhancement, which can be determined via measuring the decay times of a

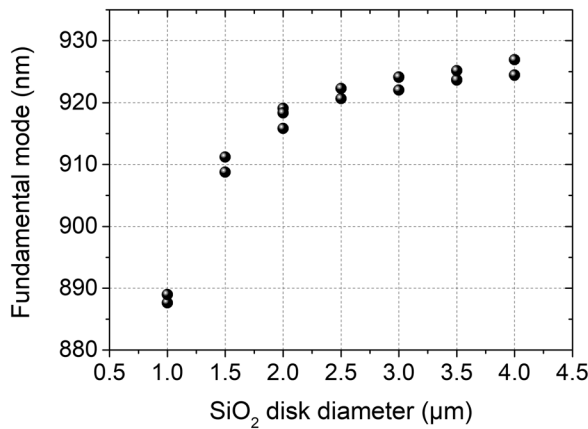


FIG. 3. Measured fundamental cavity mode for truncated Gaussian-shaped cavities realized with etching masks of different diameters. All structures have been etched for the same time.

quantum emitter inside the cavity, spectrally on and off resonance. For this purpose, a quantum dot exhibiting multiple emission lines, and spatially within a cavity is analyzed. Here, temperature tuning is used to change the spectral overlap between emission lines and cavity mode [see Fig. 4(a)]. For the cavity mode, a small red-shift with increasing temperature is observed, whereas the quantum dot emission lines all undergo a similar larger shift.

While at 4 K a charged transition (T) is close to resonance with the cavity mode, at 36 K a spectral separation is present and the

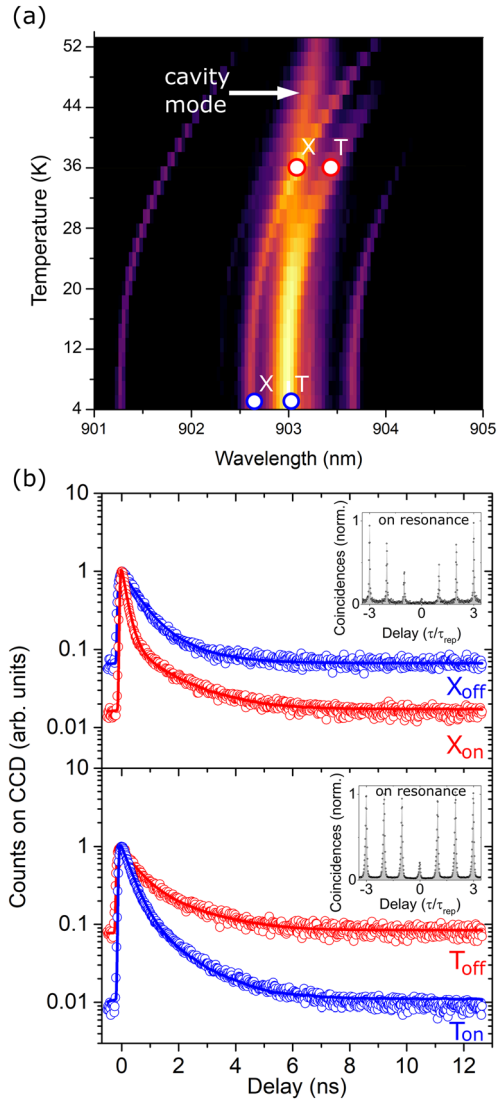


FIG. 4. (a) Quantum dot micro-photoluminescence as a function of temperature. As the QD emission lines shift stronger with temperature than the cavity resonance, they are tuned on- and off-resonance. Blue and red circles indicate the measurement points of the decay times at 4K and 36 K, respectively. X corresponds to the exciton and T to the charged state. (b) Measured decay times at 4K (blue) and 36 K (red) for the exciton X and the charged state T in the upper and lower plot, respectively. The insets show the corresponding $g^{(2)}(\tau)$ measurements performed on resonance indicating the preservation of the QD single photon characteristic.

excitonic transition (X) is on resonance. At these temperatures, decay-time measurements as seen in Fig. 4(b) are performed on both lines. A clear reduction of the decay time by a factor of 1.52 ± 0.07 (T) and 3.22 ± 0.07 (X) is measured in the resonant case. Despite both lines should, in principle, undergo the same Purcell enhancement for perfect spectral matching, a difference between the on- and off-resonance ratios is observed. First, this could stem from the fact that the charged state is slightly red-shifted with respect to the cavity at 4 K and, therefore, no perfect spectral overlap is given. Furthermore, despite the low QD density, the two transitions could originate from two different QDs. Hence, the different spatial overlap for the two investigated transitions would be directly reflected in the Purcell factor. Finally, additional non-radiative decay channels that are present at higher temperatures would decrease the actual measured decay time for both transitions at the elevated temperature. While for the first two effects, the maximal achieved Purcell factor is 3.22 ± 0.07 (X), in the latter case, the two measured ratios can be seen as an upper and lower bound for the actual Purcell enhancement. Finally, second-order correlation measurements are performed to verify that single-photon emission is preserved while being resonant with the cavity. For the charged transition, a $g_{dc}^{(2)}(0)$ value of 0.288 ± 0.001 (time integrated over a full repetition and only corrected for the detector dark count) is obtained while the excitonic line at 36 K yields $g_{dc}^{(2)}(0) = 0.057 \pm 0.001$, both clearly below 0.5 even for the employed non-resonant pumping scheme. The slightly higher value for the charged transition line can most probably be attributed to an additional emission line on the right flank of the cavity mode.

In conclusion, we demonstrated the coupling of a QD to a truncated Gaussian-shaped microcavity. We developed the fabrication process, including wet-chemical etching, oxide removal, and overgrowth. The realized cavities show a splitting of the polarization eigenmodes of 29 μeV due to the slight ellipticity of the cavity. The fundamental as well as higher order modes of one exemplary cavity have been investigated, showing a clear signature of Hermite–Gaussian modes, well according to FDTD simulations. It has been shown that the fundamental cavity mode can be shifted by varying the diameter of the etching mask and hereby the width of the microlens in the cavity center to meet the desired wavelength for optimized coupling to a certain QD. Finally, emission lines of a QD spatially inside a cavity have been shifted on- and off-resonance via temperature tuning, showing a clear decrease in the measured decay time on resonance that evidences Purcell enhancement. Second-order correlation function measurements verify the single-photon nature of the emission. This work proves the feasibility of this cavity structure. In future, its performance can be improved by tuning the QD emission into resonance with the cavity mode via strain tuning. Furthermore, a deterministic process would allow for precise spatial and spectral control of a pre-selected QD within the cavity.

This work was funded by the Deutsche Forschungsgemeinschaft (DFG; German Research Foundation) via No. 431314977/GRK2642.

AUTHOR DECLARATIONS

Conflict of Interest

The authors have no conflicts to disclose.

Author Contributions

Lena Engel and Sascha Kolatschek contributed equally to this work.

Lena Engel: Data curation (lead); Formal analysis (lead); Investigation (lead); Validation (equal); Visualization (lead); Writing – original draft (lead); Writing – review & editing (supporting). **Sascha Kolatschek:** Data curation (lead); Formal analysis (lead); Investigation (lead); Validation (equal); Visualization (lead); Writing – original draft (lead); Writing – review & editing (supporting). **Thomas Herzog:** Data curation (supporting); Investigation (supporting); Writing – original draft (supporting); Writing – review & editing (supporting). **Sergej Vollmer:** Data curation (supporting); Investigation (supporting); Writing – original draft (supporting); Writing – review & editing (supporting). **Michael Jetter:** Conceptualization (equal); Project administration (equal); Resources (equal); Supervision (equal); Validation (equal); Writing – original draft (supporting); Writing – review & editing (equal). **Simone L. Portalupi:** Conceptualization (equal); Project administration (equal); Resources (equal); Supervision (equal); Validation (equal); Writing – original draft (supporting); Writing – review & editing (equal). **Peter Michler:** Conceptualization (equal); Project administration (equal); Resources (equal); Supervision (equal); Validation (equal); Writing – original draft (supporting); Writing – review & editing (equal).

DATA AVAILABILITY

The data that support the findings of this study are available from the corresponding author upon reasonable request.

REFERENCES

- ¹N. Tomm, A. Javadi, N. O. Antoniadis, D. Najer, M. C. Löbl, A. R. Korsch, A. D. Wieck, A. Ludwig, and R. J. Warburton, “A bright and fast source of coherent single photons,” *Nat. Nanotechnol.* **16**, 399–403 (2021).
- ²H. Wang, Y.-M. He, T.-H. Chung, Y. Hu, H. Yu, S. Chen, X. Ding, M.-C. Chen, J. Qin, X. Yang, R.-Z. Liu, Z.-C. Duan, J.-P. Li, S. Gerhardt, K. Winkler, J. Jurkat, N. Gregersen, Y.-H. Huo, Q. Dai, S. Yu, S. A. Höfling, C.-Y. Lu, and J.-W. Pan, “Towards optimal single-photon sources from polarized microcavities,” *Nat. Photonics* **13**, 770–775 (2019).
- ³E. Knill, R. Laflamme, and G. J. Milburn, “A scheme for efficient quantum computation with linear optics,” *Nature* **409**, 46–52 (2001).
- ⁴N. Gisin, G. Ribordy, W. Tittel, and H. Zbinden, “Quantum cryptography,” *Rev. Mod. Phys.* **74**, 145–195 (2002).
- ⁵S. Strauf, “Towards efficient quantum sources,” *Nat. Photonics.* **4**, 132–134 (2010).
- ⁶W. Barnes, G. Björk, J. Gérard, P. Jonsson, J. Wasey, P. Worthing, and V. Zwiller, “Solid-state single photon sources: Light collection strategies,” *Eur. Phys. J. D - At. Mol. Opt. Plasma Phys.* **18**(2), 197–210 (2002).
- ⁷M. Sartison, S. L. Portalupi, T. Gissibl, M. Jetter, H. Giessen, and P. Michler, “Combining *in-situ* lithography with 3D printed solid immersion lenses for single quantum dot spectroscopy,” *Sci. Rep.* **7**, 39916 (2017).
- ⁸M. Gschrey, A. Thoma, P. Schnauber, M. Seifried, R. Schmidt, B. Wohlfeil, L. Krüger, J. H. Schulze, T. Heindel, S. Burger, F. Schmidt, A. Strittmatter, S. Rodt, and S. Reitzenstein, “Highly indistinguishable photons from deterministic quantum-dot microlenses utilizing three-dimensional *in situ* electron-beam lithography,” *Nat. Commun.* **6**, 7662 (2015).
- ⁹Y. Chen, M. Zopf, R. Keil, F. Ding, and O. G. Schmidt, “Highly-efficient extraction of entangled photons from quantum dots using a broadband optical antenna,” *Nat. Commun.* **9**, 2994 (2018).
- ¹⁰M. Munsch, N. S. Malik, E. Dupuy, A. Delga, J. Bleuse, J.-M. Gérard, J. Claudon, N. Gregersen, and J. Mørk, “Dielectric GaAs antenna ensuring and

- efficient broadband coupling between an InAs quantum dot and a Gaussian optical beam,” *Phys. Rev. Lett.* **110**, 177402 (2013).
- ¹¹J. Claudon, J. Bleuse, N. S. Malik, M. Bazin, P. Jaffrennou, N. Gregersen, C. Sauvan, P. Lalanne, and J.-M. Gérard, “A highly efficient single-photon source based on a quantum dot in a photonic nanowire,” *Nat. Photonics* **4**, 174 (2010).
- ¹²N. Somaschi, V. Giesz, L. De Santis, J. C. Loredó, M. P. Almeida, G. Hornecker, S. L. Portalupi, T. Grange, C. Antón, J. Demory, C. Gómez, I. Sagnes, N. D. Lanzillotti-Kimura, A. Lemaître, A. Auffèves, A. G. White, L. Lanco, and P. Senellart, “Near-optimal single-photon sources in the solid state,” *Nat. Photonics* **10**, 340 (2016).
- ¹³H. Wang, Z.-C. Duan, Y.-H. Li, S. Chen, J.-P. Li, Y.-M. He, M.-C. Chen, Y. He, X. Ding, C.-Z. Peng, C. Schneider, M. Kamp, S. Höfling, C.-Y. Lu, and J.-W. Pan, “Near-transform-limited single photons from an efficient solid-state quantum emitter,” *Phys. Rev. Lett.* **116**, 213601 (2016).
- ¹⁴P. Michler, A. Kiraz, C. Becher, W. V. Schoenfeld, P. M. Petroff, L. Zhang, E. Hu, and A. Imamoglu, “A quantum dot single-photon turnstile device,” *Science* **290**(5500), 2282–2285 (2000).
- ¹⁵T. Steinmetz, Y. Colombe, D. Hunger, T. W. Hänsch, A. Balocchi, R. J. Warburton, and J. Reichel, “Stable fiber-based Fabry-Pérot cavity,” *Appl. Phys. Lett.* **89**, 111110 (2006).
- ¹⁶M. Davanço, M. T. Rakher, D. Schuh, A. Badolato, and K. Srinivasan, “A circular dielectric grating for vertical extraction of single quantum dot emission,” *Appl. Phys. Lett.* **99**(4), 041102 (2011).
- ¹⁷S. Kolatschek, S. Hepp, M. Sartison, M. Jetter, P. Michler, and S. L. Portalupi, “Deterministic fabrication of circular Bragg gratings coupled to single quantum emitters via the combination of *in-situ* optical lithography and electron-beam lithography,” *J. Appl. Phys.* **125**, 045701 (2019).
- ¹⁸D. Englund, D. Fattal, E. Waks, G. Solomon, B. Zhang, T. Nakaoka, Y. Arakawa, Y. Yamamoto, and J. Vučković, “Controlling the spontaneous emission rate of single quantum dots in a two-dimensional photonic crystal,” *Phys. Rev. Lett.* **95**, 013904 (2005).
- ¹⁹K. Hennessy, A. Badolato, M. Winger, D. Gerace, M. Atatüre, S. Gulde, S. Fält, E. L. Hu, and A. Imamoglu, “Quantum nature of a strongly coupled single quantum dot-cavity system,” *Nature* **445**, 896 (2007).
- ²⁰C. Nawrath, R. Joos, S. Kolatschek, S. Bauer, P. Pruy, F. Hornung, J. Fischer, J. Huang, P. Vijayan, R. Sittig, M. Jetter, S. L. Portalupi, and P. Michler, “High emission rate from a Purcell-enhanced, triggered source of pure single photons in the telecom c-band,” [arXiv:2207.12898](https://arxiv.org/abs/2207.12898) (2022).
- ²¹H. Benisty, H. De Neve, and C. Weisbuch, “Impact of planar microcavity effects on light extraction-Part I: Basic concepts and analytical trends,” *IEEE J. Quantum Electron.* **34**(9), 1612–1631 (1998).
- ²²E. Daïf, A. Baas, T. Guillet, J.-P. Brantut, R. Idrissi Kaitouni, J. L. Staehli, F. Morier-Genoud, and B. Deveaud, “Polariton quantum boxes in semiconductor microcavities,” *Appl. Phys. Lett.* **88**, 061105 (2006).
- ²³P. Lugan, D. Sarchi, and V. Savona, “Theory of trapped polaritons in patterned microcavities,” *Phys. Status Solidi C* **3**, 2428–2431 (2006).
- ²⁴F. Ding, T. Stöferle, L. Mai, A. Knoll, and R. F. Mahrt, “Vertical microcavities with high q and strong lateral mode confinement,” *Phys. Rev. B* **87**, 161116 (2013).
- ²⁵L. Mai, F. Ding, T. Stöferle, A. Knoll, B. J. Offrein, and R. F. Mahrt, “Integrated vertical microcavity using a nano-scale deformation for strong lateral confinement,” *Appl. Phys. Lett.* **103**, 243305 (2013).
- ²⁶R. Trotta, E. Zallo, C. Ortix, P. Atkinson, J. D. Plumhof, J. van den Brink, A. Rastelli, and O. G. Schmidt, “Universal recovery of the energy-level degeneracy of bright excitons in InGaAs quantum dots without a structure symmetry,” *Phys. Rev. Lett.* **109**, 147401 (2012).
- ²⁷E. Koroknay, W.-M. Schulz, U. R. M. Richter, D. Rengstl, M. Bommer, C. A. Kessler, R. Roßbach, H. Schweizer, M. Jetter, and P. Michler, “Vertically stacked and laterally ordered InP and In(Ga)As quantum dots for gate applications,” *Phys. Status Solidi B* **249**, 737 (2012).
- ²⁸M. Sartison, L. Engel, S. Kolatschek, F. Olbrich, C. Nawrath, S. Hepp, M. Jetter, P. Michler, and S. L. Portalupi, “Deterministic integration and optical characterization of telecom o-band quantum dots embedded into wet-chemically etched Gaussian-shaped microlenses,” *Appl. Phys. Lett.* **113**(3), 032103 (2018).
- ²⁹H. Asai, “Anisotropic lateral growth in GaAs MOCVD layers on (001) substrates,” *J. Cryst. Growth* **80**(2), 425–433 (1987).
- ³⁰C. Bonato, J. Gudat, T. S. de Vries, M. Keesjan, H. Kim, P. M. Petroff, M. P. van Exter, and D. Bouwmeester, “Optical modes in oxide-apertured micropillar cavities,” *Opt. Lett.* **37**, 4678–4680 (2012).
- ³¹J. M. Gérard, D. Barrier, J. Y. Marzin, R. Kuszelwicz, L. Manin, E. Costard, V. Thierry-Mieg, and T. Rivera, “Quantum boxes as active probes for photonic microstructures: The pillar microcavity case,” *Appl. Phys. Lett.* **69**, 449 (1996).